Adaptive resolution simulations of biomolecular systems

Julija Zavadlav, Staš Bevc & Matej Praprotnik

European Biophysics Journal
with Biophysics Letters

ISSN 0175-7571
Volume 46
Number 8

Eur Biophys J (2017) 46:821-835
DOI 10.1007/s00249-017-1248-0

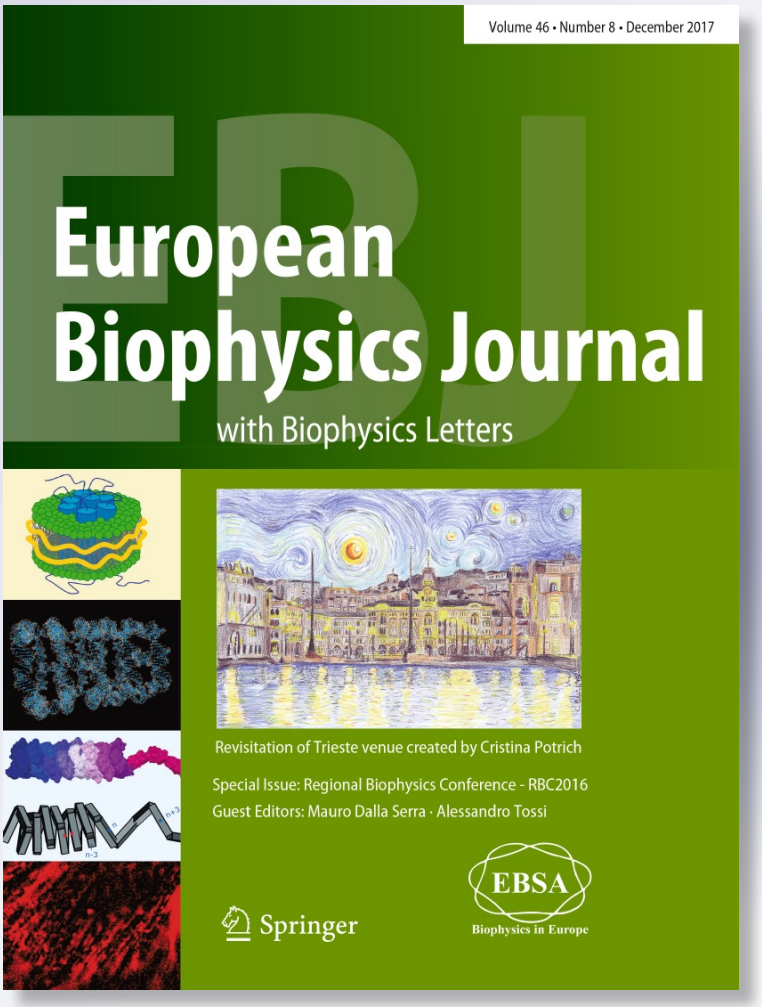

Springer

Eur Biophys J (2017) 46:821–835
DOI 10.1007/s00249-017-1248-0

REVIEW

EBSA
Biophysics in Europe

Adaptive resolution simulations of biomolecular systems

Julija Zavadlav[1,2,3] · Staš Bevc[1] · Matej Praprotnik[1,2]

Received: 28 February 2017 / Revised: 12 June 2017 / Accepted: 15 August 2017 / Published online: 13 September 2017

Abstract In this review article, we discuss and analyze some recently developed hybrid atomistic–mesoscopic solvent models for multiscale biomolecular simulations. We focus on the biomolecular applications of the adaptive resolution scheme (AdResS), which allows solvent molecules to change their resolution back and forth between atomistic and coarse-grained representations according to their positions in the system. First, we discuss coupling of atomistic and coarse-grained models of salt solution using a 1-to-1 molecular mapping—i.e., one coarse-grained bead represents one water molecule—for development of a multiscale salt solution model. In order to make use of coarse-grained molecular models that are compatible with the MARTINI force field, one has to resort to a supramolecular mapping, in particular to a 4-to-1 mapping, where four water molecules are represented with one coarse-grained bead. To this end, bundled atomistic water models are employed, i.e., the relative movement of water molecules that are mapped to the same coarse-grained bead is restricted by employing harmonic springs. Supramolecular coupling has recently also been extended to polarizable coarse-grained water models with explicit charges. Since these coarse-grained models consist of several interaction sites, orientational degrees of freedom of the atomistic and coarse-grained representations are coupled via a harmonic energy penalty term. The latter aligns the dipole moments of both representations. The reviewed multiscale solvent models are ready to be used in biomolecular simulations, as illustrated in a few examples.

Keywords Molecular dynamics · Adaptive resolution · Supramolecular coupling

Special Issue: Regional Biophysics Conference 2016.

✉ Matej Praprotnik
praprot@cmm.ki.si

[1] Department of Molecular Modeling, National Institute of Chemistry, Hajdrihova 19, 1001 Ljubljana, Slovenia

[2] Department of Physics, Faculty of Mathematics and Physics, University of Ljubljana, Jadranska 19, 1000 Ljubljana, Slovenia

[3] Chair of Computational Science, ETH Zurich, Clausiusstrasse 33, 8092 Zurich, Switzerland

Introduction

Molecular simulations have become a well-established and indispensable tool for studies of complex phenomena in soft and biological matter (Frenkel and Smit 2001; Allen and Tildesley 1989; Tuckerman 2010). They provide detailed insight into structural as well as functional properties of biological macromolecules that are sometimes too difficult to obtain experimentally or too complex to be treated theoretically (Karplus and McCammon 2002; Chopraa et al. 2008; Kamerlin et al. 2011). Biomolecular systems are, however, very challenging to simulate, because they are characterized by physical properties that are determined by the interplay of disparate spatiotemporal scales. This inevitably leads to a trade-off between efficiency and accuracy. Atomistic (AT) molecular dynamics (MD) simulations can describe a system in great detail but are computationally expensive. Despite the increasing computational power and ongoing efforts to enhance the efficiency of MD algorithms (Shaw et al. 2007), they are often incapable of spanning the time and length scales required for solutions of important problems.

On the other hand, with systematic coarse-graining techniques (Noid 2013; Rudzinski and Noid 2015; Zhou 2014; Ingólfsson et al. 2014; Marrink et al. 2007; Peter and Kremer 2009; Lyubartsev and Laaksonen 1995; Reith et al. 2003;

Ayton et al. 2007; Izvekov and Voth 2005b; Mullinax and Noid 2009; Shell 2008; Carmichael and Shell 2012; Foley et al. 2015), where several atoms are grouped together into effective interaction sites, efficiency can be increased up to several orders of magnitude. A wide range of coarse-grained (CG) models already exist for different biomolecules, including proteins (Bereau and Deserno 2009; Chebaro et al. 2012; Monticelli et al. 2008; Basdevant et al. 2007), nucleic acids (Hinckley et al. 2014; Lyubartsev et al. 2015; Gonzales et al. 2013; Dans et al. 2016; Uusitalo et al. 2015; Savelyev and Papoian 2010; Ouldridge et al. 2011; Snodin et al. 2015; Maciejczyk et al. 2014; Maffeo et al. 2014; Cragnolini et al. 2013; Gopal et al. 2010; Knotts et al. 2007; Dans et al. 2010), and lipid bilayers (Shelley et al. 2001; Marrink et al. 2007; Orsi and Essex 2011; Izvekov and Voth 2005a, 2006; Kranenburg et al. 2004; Wang and Deserno 2010; Reynwar et al. 2007). Nevertheless, due to the inherent simplifications, this large gain commonly comes at the cost of reduced accuracy of the CG model relative to the AT model (Foley et al. 2015).

Multiscale simulations have emerged as a promising tool for such problems, as they overcome the limitations of both AT and CG simulations by providing not only computational advantages but also enhanced insight. A variety of multiscale simulation methods have been proposed, and they can be classified into two groups: sequential and concurrent approaches (Goga et al. 2009; Potestio et al. 2013; Wassenaar et al. 2013; Neri et al. 2005; Rzepiela et al. 2011; Han and Schulten 2012; Sokkar et al. 2013; Gonzales et al. 2013; Shi et al. 2006). In the sequential methods, the entire system is treated on one level of resolution at a time (Harmandarisab and Kremer 2009; Harmandarisab et al. 2006; Izvekov et al. 2004; Lyubartsev and Laaksonen 1995; Lyubartsev 2005; Lyubartsev et al. 2015). The information obtained at a higher level of resolution is used, for example, to parameterize a lower-resolution model. Back-mapping methods allow switching between the different levels of resolution, i.e., reintroducing the chemical details whenever needed (Wassenaar et al. 2015; Tschöp et al. 1998; Hess et al. 2006). By contrast, in concurrent methods, multiple levels of resolution are applied at the same time within one simulation (Orsi et al. 2014; Shen and Hu 2014; Rzepiela et al. 2011; Shi et al. 2006; Shen and Yang 2016; Mohamed and Mohamad 2010; Fabritiis et al. 2006; Fedosov et al. 2009; Walther et al. 2012; Nielsen et al. 2010; Heyden and Truhlar 2008; Sokkar et al. 2015; Cameron 2005; Alekseevaa et al. 2016; Potestio et al. 2014).

Among the advanced multiscale methods is the Adaptive Resolution Scheme (AdResS) (Praprotnik et al. 2005, 2008, 2011), which can successfully couple two or more levels of resolution simultaneously present in the system. A key feature of AdResS is that the particles can change their resolution on the fly during the course of an MD simulation. The method is tailor-made for systems where AT resolution is required only in a spatially localized region, whereas a lower CG level of detail is sufficient for the rest of the system. Such cases are typically found in simulations of complex biophysical macromolecules such as deoxyribonucleic acid (DNA), proteins, and lipid membranes. There, the AT resolution is required only for the macromolecule and the solvent in its vicinity, whereas the solvent farther away is adequately treated on a simplified CG level. The original version of the AdResS based on force coupling does not allow for a definition of a Hamiltonian, and consequently must be employed in conjunction with a thermostat. A recent Hamiltonian version of the method, the H-AdResS (Potestio et al. 2013; Kreis et al. 2014; Español et al. 2015), on the other hand, allows for definition of a global Hamiltonian, which enables one to perform adaptive resolution Monte Carlo simulations (Potestio et al. 2013). However, as the translation invariance is broken due to the resolution change, this implies that the total linear momentum cannot be conserved by H-AdResS. Because the conservation of linear momentum is crucial for hydrodynamics, the original AdResS—which is not Hamiltonian, and thus can preserve linear momentum despite broken translational symmetry—is more convenient for coupling with continuum hydrodynamics (Delgado-Buscalioni et al. 2008, 2009). Recent extensions of AdResS also involve coupling to a quantum level of description (Poma and Delle Site 2010, 2011; Agarwal and Delle 2015, 2016) as well as to open systems that exchange mass, momentum, and energy with their surroundings (Delgado-Buscalioni et al. 2015a, b; Sablić et al. 2016; Wang et al. 2013; Agarwal et al. 2014; Wang and Agarwal 2015; Delle Site 2016; Mukherji et al. 2013; Kreis et al. 2015). This allows for performing MD simulations either in a grand-canonical statistical ensemble or under non-equilibrium conditions (Delgado-Buscalioni et al. 2015a; Sablić et al. 2016). In this review, however, we will focus on recent applications of AdResS to biomolecular systems such as proteins (Zavadlav et al. 2014b; Fogarty et al. 2015) and DNA molecules (Zavadlav et al. 2015b, 2016b) solvated in multiscale solvents (Bevc et al. 2013; Nagarajan et al. 2013; Zavadlav et al. 2014a, 2015a).

Adaptive resolution simulation

To conduct adaptive resolution MD simulations, we resort to AdResS (Praprotnik et al. 2005, 2008, 2011). AdResS is a multiscale MD method that allows concurrent coupling between two domains, where MD simulations can be performed by different force fields. Hence the method can couple the high and low levels of detail, and it can also be applied to systems with domains that are described with different models of the same resolution. A key feature of the AdResS method is that it allows molecules to freely move

across different regions and change their resolution on the fly according to their position in the computational domain. When a CG molecule leaves the CG domain, it is remapped into the atomistically resolved molecule with a random orientation. To avoid any overlaps of its atoms with the atoms of the neighboring molecules, the introduction of the AT degrees of freedom must be continuous and not instantaneous. To this end, an interface layer between the AT and CG regions is introduced that allows an AT molecule to gradually find an energetically permissible orientation relative to its neighboring molecules. This transition region, also called a hybrid (HY) region, contains hybrid molecules where both representations are superimposed.

The coupling is achieved via a force interpolation scheme. The total force on the molecule—or bundle in cases where a 4-to-1 mapping is used—α is given by

$$\mathbf{F}_\alpha = \sum_{\beta\neq\alpha} w(|\mathbf{R}_\alpha - \mathbf{R}|)w(|\mathbf{R}_\beta - \mathbf{R}|)\mathbf{F}^{\mathrm{AT}}_{\alpha\beta} + \sum_{\beta\neq\alpha}[1 - w(|\mathbf{R}_\alpha - \mathbf{R}|)w(|\mathbf{R}_\beta - \mathbf{R}|)]\mathbf{F}^{\mathrm{CG}}_{\alpha\beta} - \mathbf{F}^{\mathrm{TD}}_\alpha(|\mathbf{R}_\alpha - \mathbf{R}|), \quad (1)$$

where w is a weighting function that governs the transition between regions of different resolution, and therefore needs to be smooth. This function depends on the position of the mapping point of the molecule (bundle) and is defined as follows: $w = 1$ corresponds to the AT region, and $w = 0$ to the CG region, whereas the values $0 < w < 1$ correspond to the HY region.

This method can accommodate various geometric boundaries between the resolution regions. In examples presented in this review, we demonstrate splittings in one direction (Zavadlav et al. 2014a), cylinder (Zavadlav et al. 2015b), and a sphere (Zavadlav et al. 2014b). The relative vector $\mathbf{R}_\alpha - \mathbf{R}$ is correspondingly a one-, two-, or three-dimensional vector from the molecule's position to the center of the AT region denoted by $\mathbf{R}$. The geometrical boundary between resolution regions can thus be set to reflect the shape of the simulated molecule, i.e., cylindrical for DNA molecules and spherical for proteins. It can be even self-adjusting (Kreis et al. 2016). The center of the AT region can either be a fixed point (usually the center of the simulation box) or a mobile point, as in a simulation of a macromolecule, for example, where it coincides with the macromolecule's center of mass. A setup where the center of the AT region follows the macromolecule's random translation ensures that the macromolecule is always expressed in full all-atom detail and surrounded by a layer of all-atom solvent. Alternatively, we can also use AdResS to tackle problems where a macromolecule spreads over several resolution regions (Praprotnik et al. 2011; Fogarty et al. 2016; Peters et al. 2016).

In general, the AT and CG representations can differ substantially in thermodynamical properties such as pressure and chemical potential. Pressure differences at the transition boundaries introduce a spurious drift force on the molecules that cause them to migrate into a region with lower chemical potential. This leads to density variations in the system. To compensate such spurious effects, an external thermodynamic (TD) force $\mathbf{F}^{\mathrm{TD}}_\alpha$ opposing the chemical potential gradient is applied on molecules (bundles) with mass M in the transition region (Poblete et al. 2010; Fritsch et al. 2012; Praprotnik et al. 2011). The TD force is calculated in an iterative manner as (Fritsch et al. 2012):

$$\mathbf{F}^{\mathrm{TD}}_{\alpha\ i+1} = \mathbf{F}^{\mathrm{TD}}_{\alpha\ i} - \frac{M}{\rho_0^2\kappa_T}\nabla\rho_i(\mathbf{r}), \quad (2)$$

where ρ_0 and κ_T are the bulk density and isothermal compressibility, respectively. The iteration is performed until the system obtains the uniform target density. In practice, however, we use the formula (Praprotnik et al. 2011):

$$\mathbf{F}^{\mathrm{TD}}_{\alpha\ i+1} = \mathbf{F}^{\mathrm{TD}}_{\alpha\ i} - C_i\nabla\rho_i(\mathbf{r}), \quad (3)$$

where C is a numerical prefactor that is determined empirically. The value of the prefactor is adjusted along the process to prevent overcorrection. To speed up the iteration procedure, we also run several simulations with different prefactors simultaneously at each step, and choose the best for the next iteration. In addition, when different types of particles are present in the system, the iteration procedure is applied for all types. On the other hand, if the CG representation is chosen to be equal to the AT representation (this corresponds to a fully AT system), then $\mathbf{F}^{\mathrm{TD}}_\alpha = 0$ and Eq. (1) is simplified to $\mathbf{F}_\alpha = \sum_{\beta\neq\alpha}\mathbf{F}^{\mathrm{AT}}_{\alpha\beta}$.

AdResS simulations discussed in this review were performed using the ESPResSo++ software package (Halverson et al. 2013). A local Langevin thermostat was employed to maintain a constant temperature of 300 K. The periodic boundary conditions were employed in all three directions, together with the minimum image convention (Allen and Tildesley 1989). The non-bonded interactions were calculated explicitly within a cutoff distance. The electrostatic interactions beyond the cutoff were treated with either the reaction field (RF) (Neumann 1985, 1983) or generalized reaction field (GRF) correction (Tironi et al. 1995). Remaining computational details are provided in Zavadlav et al. (2014a, b, 2015a, b). In the remainder of this review, we will describe recent efforts to apply this and similar multiscale methodologies for the simulation of biomolecular systems.

Multiscale solvents

In multiscale simulations of biophysical systems, one can treat biomacromolecules at multiple scales, so that different

parts of the macromolecules are modeled using different resolutions (see, e.g., Delle Site et al. 2002; Villa et al. 2004, 2005; Neri et al. 2005; Praprotnik et al. 2011; Machado et al. 2011; Machado and Pantano 2015). Here, we will not dwell upon this kind of approach. Instead, since the majority of the computational time is consumed by simulating the dynamics of a solvent, we will focus on the treatment of the solvent around the biomolecules at multiple scales. We begin with a 1-to-1 mapping. In terms of water, that means that each water molecule is represented with a single site (Praprotnik et al. 2007; Matysiak et al. 2008; Lu et al. 2014). Because this coarse-graining strategy offers rather limited speedup, we next discuss a 4-to-1 supramolecular mapping, where an AT model is linked to the non-polarizable and polarizable MARTINI water models (Marrink et al. 2007; Monticelli et al. 2008). Difficulties that arise from coupling to a CG model with supramolecular mapping can be successfully circumvented by using bundled water models. The same approach can be extended to other supramolecular mappings, depending on the supramolecular CG water model employed. For example, one of the most promising supramolecular CG water models is that described by Riniker and Gunsteren (2011), with a 5-to-1 supramolecular mapping.

Salt solution: 1-to-1 molecular mapping

We start off by briefly describing our published derivation of a multiscale salt solution model (Bevc et al. 2013; Zavadlav et al. 2015b). First, we parameterized a CG model to reproduce structural properties of the AT model [AMBER force field (Duan et al. 2003) for ions and TIP3P (Jorgensen et al. 1983) water model]. The spherically symmetrical effective potentials for the water–water, water–sodium (Na^+), and water–chloride (Cl^-) interactions (shown in Fig. 1) are obtained using the iterative Boltzmann inversion method (Reith et al. 2003), which is incorporated into the STructure mapper and Online Coarse-graining Kit (STOCK) web toolkit (Bevc et al. 2015).

In these calculations, we have employed the GRF method (Tironi et al. 1995) for the electrostatic interaction beyond the cutoff, with the dielectric permittivity of the outer region equal to 80 and the inverse Debye screening length $\kappa = 3.25\,\mathrm{nm}^{-1}$ corresponding to a 1 M salt solution. The dielectric permittivity of the inner region, i.e., within the cutoff distance, is equal to 1 and 80 for the AT and CG regions, respectively. This ensures that the ion–ion interactions are properly screened in the CG region, where we use the same electric charges for the salt ions as in the AT region; thus, aside from the change in dielectric permittivity, the ions interact via the same potentials in the AT and CG models.

The correct local structure is obtained in the subdomains (labeled AdResS AT and AdResS CG) of the AdResS simulation, where only the molecules in the corresponding region are taken into consideration.

To compensate for the difference in the chemical potential at different levels of resolution, and to achieve a uniform density profile throughout the simulation box, we have applied the TD forces. They act mostly in the HY region and are obtained with an iterative procedure as described by Praprotnik et al. (2011) and Fritsch et al. (2012). Figure 2 shows the TD forces used for the water molecule and sodium and chloride ions.

The normalized density profiles (NDPs) for the corresponding molecule types are computed along the direction of the resolution change, i.e., as a function of the distance

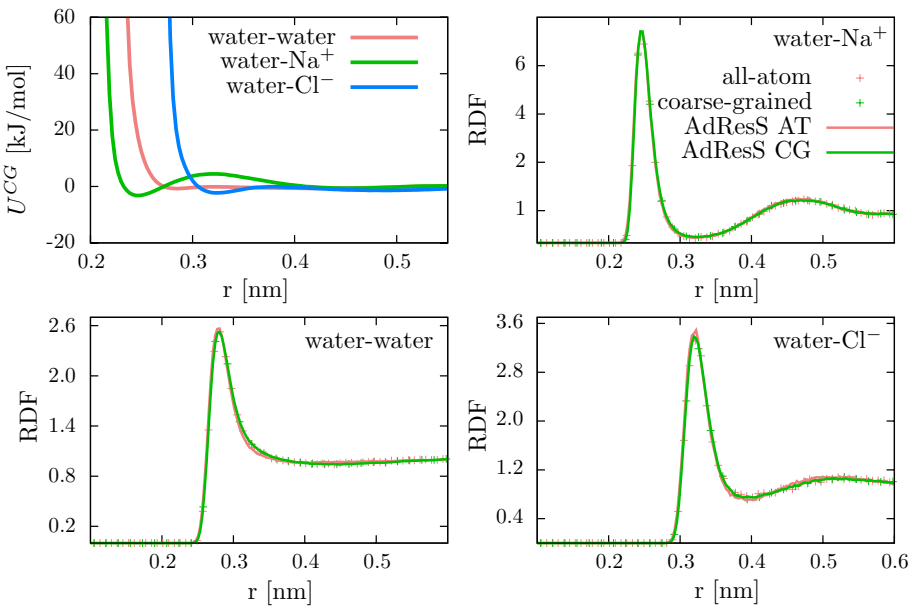

Fig. 1 Effective pair potential interactions between center of mass of molecules for water–water, water–Na^+ and water–Cl^- and the corresponding radial distribution functions (RDFs). The all-atom RDFs are well reproduced by the fully CG and AdResS simulations in both the AT (AdResS AT) and CG (AdResS CG) regions. Adapted with permission from (Zavadlav et al. 2015b). Copyright 2015 American Chemical Society

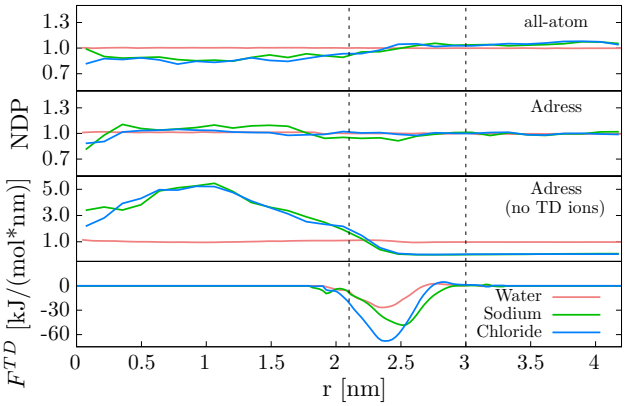

Fig. 2 Normalized density profile for the center-of-mass water molecules and sodium and chloride ions. The results are shown for the all-atom simulation and AdResS simulations. For comparison, the results from additional AdResS simulation are shown, where TD force is added only to water molecules. The *bottom plot* shows the TD forces applied to all three molecule types. *Vertical dotted lines* denote boundaries of the HY region. Adapted with permission from Zavadlav et al. (2015b). Copyright 2015 American Chemical Society

from the center of the AT region. The results are shown for three simulations: all-atom, AdResS with thermodynamic forces acting on all molecule types, and AdResS with thermodynamic forces acting on water molecules only. The TD force (see Fig. 2) is able to flatten the density profile substantially. Larger deviations from the ideally flat profile are seen for the ions, due to the lower number of ions in the system compared to the water. However, these deviations are comparable to those obtained from the all-atom simulation. The TD force for bundles can be iterated independently of the TD forces of ions. This can be observed from the NDPs of the AdResS simulation where the TD force is acting only on bundles. In contrast, both Na^+ and Cl^- TD forces must be iterated simultaneously, since the density distributions of Na^+ and Cl^- are mutually dependent (Bevc et al. 2013).

Supramolecular water: 4-to-1 molecular mapping

Next, we turn our attention to the multiscale water model (Zavadlav et al. 2014a) with a 4-to-1 mapping, where AT water, composed of a bundle of four simple point charge (SPC) water molecules (Fuhrmans et al. 2010), is coupled to the MARTINI CG water (Marrink et al. 2007), as illustrated in Fig. 3.

The system is split along the x-axis, so that an AT domain is at the center of the simulation box. Two HY regions flank the AT region. The bundle molecules change their resolution

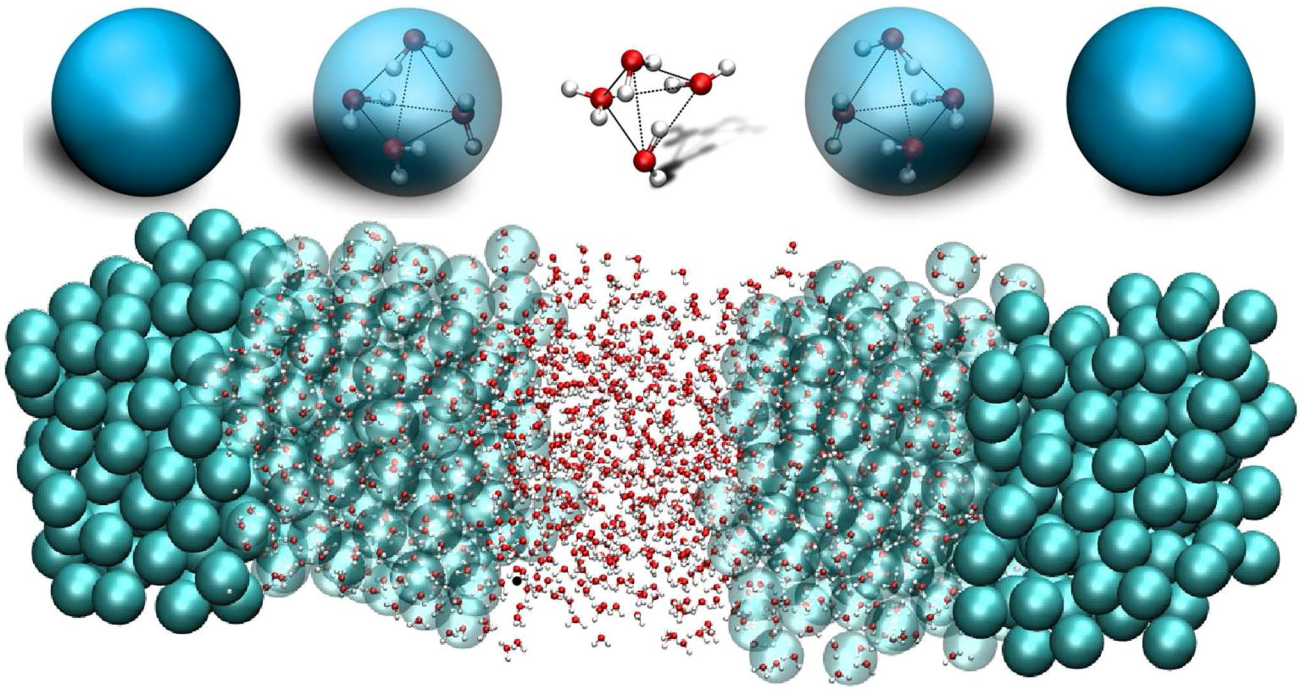

Fig. 3 *Bottom*: depiction of a supramolecular water AdResS system with resolution changing from AT (*center*) to CG (*edges*); the molecules change their representation on the fly as they diffuse through the transition HY regions. *Top*: illustration of different resolutions for an individual water cluster; in the AT region, the bundled-SPC water model (Fuhrmans et al. 2010) is used, where four SPC water oxygen atoms are connected by semi-harmonic springs; in the CG region, the four water molecules are grouped into a single particle with MARTINI (Marrink et al. 2007) water model parameters. Figure reprinted from Zavadlav (2015)

between the AT and CG representations on the fly in accordance with their positions in the system.

The mapping of several small molecules into a single CG site introduces new challenges to the AdResS simulations. The scheme accomplishes multiscaling by treating the system at both levels of detail simultaneously, and requires a mapping between the AT and CG representations. Thus far, the mapping has been rather straightforward, as the coordinates of CG beads were set to be identical to the center of mass of the corresponding AT atoms. However, such correspondence cannot be used in the case of supramolecular mapping, because the center of mass of AT molecules becomes meaningless when they diffuse too far away from each other. For example, in the case of water, it is known that the lifetime of tetrahedral clusters in water is well below 1 ps (Praprotnik et al. 2008). Consequently, multiple water molecules cannot be easily coupled to a single CG particle, as such coupling would require water molecules to be redistributed into CG beads on the fly.

Coupling can be simplified with a constant mapping, i.e., CG particles are mapped to the same four water molecules during the entire simulation run. In this case it is necessary to restrict the relative movement of water molecules within the bundle so that they remain first neighbors. To this end, we have resorted to a bundled AT water model introduced by Fuhrmans et al. (2010). The bundling is achieved via the introduction of attractive harmonic potentials between all oxygen pairs in a bundle, causing the bundles to adopt a roughly tetrahedral shape. The potential has the following form:

$$U^{\mathrm{AT}}_{\mathrm{spring}} = \begin{cases} \frac{1}{2}k_{\mathrm{s}}(r_{ij} - r_0)^2, & r_{ij} > r_0 \\ 0, & r_{ij} < r_0 \end{cases}, \tag{4}$$

where k_{s} represents the force constant, r_{ij} the distance between oxygen atoms, and r_0 the equilibrium distance between oxygen atoms. We used modified oxygen–oxygen Lennard-Jones (LJ) parameters that were developed for the bundled models to reproduce the properties of SPC water (Fuhrmans et al. 2010). In the CG region, the water bundles are modeled with the MARTINI force field as single particles. By using the bundled water as our AT water model, we avoid theoretical difficulties of both the AdResS (Praprotnik et al. 2008) and CG water models with several molecules per CG bead (Bock et al. 2007), i.e., the mapping of the bundled water to the MARTINI model corresponds effectively to the 1-to-1 mapping.

To validate the coupling, we have assessed the relevant statistical properties of the system, e.g., RDFs, and confirmed that the local structure in AdResS domains is the same as in the reference AT/CG simulations (Zavadlav et al. 2014a). For instance, when AT water molecules approach a neutral fluid surface (as happens upon entering the CG water region), the hydrogen bond network formed among the AT molecules can be strongly perturbed. As a result, the AT molecules near the resolution interface can orient and behave differently from the bulk. However, this spurious effect can be avoided by using an appropriate HY domain between the AT and CG domains. Studies have shown that this perturbation extends around 1 nm into the AT water layer (Jedlovszky et al. 2007; Praprotnik et al. 2007). This distance is smaller than the width of our HY region.

Figure 4 shows the average orientations of three vectors, namely the dipole moment of a water molecule, the vector joining the two hydrogen atoms of the molecule, and the vector perpendicular to the plane of the molecule, as a function of coordinate x spanning the two resolutions in the simulation box. We denote the angles formed by these vectors and the normal vector pointing toward our CG water liquid as α, β, and γ, respectively. The average orientations of the vectors are quantified by the average cosines of these angles (Zavadlav et al. 2014a). Note that a random orientation corresponds to $\cos\alpha = 0.0$ and $\cos\beta = \cos\gamma = 0.5$. The difference is due to physically indistinguishable opposite directions for the vector perpendicular to the plane of the molecule and the vector joining the two hydrogen atoms, whereas the dipole vector has a specific directionality (Praprotnik et al. 2007). The results (Fig. 4) demonstrate that after crossing the HY region, the water molecules have a random orientation in the AT domain. The molecules are slightly anisotropically oriented in the HY region. The HY region, however, is large enough to neutralize the orientational effect of the CG domain so that the water in the AT region has the same structural properties as the all-atom bulk water.

The plot of the time evolution of a diffusion profile of the bundled water molecules' center of mass, Fig. 5,

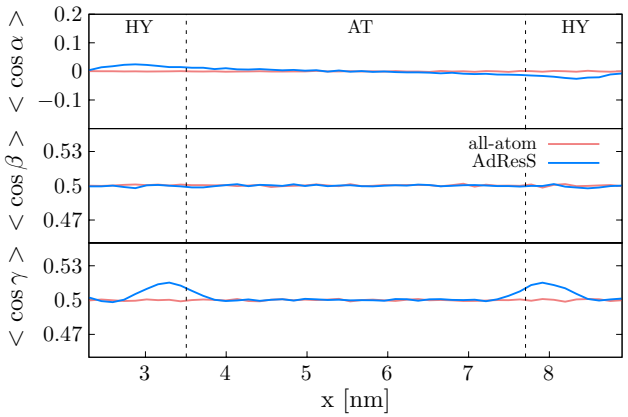

Fig. 4 Average cosine of the angle formed by the dipole vector (*top panel*), the vector joining the two hydrogen atoms of a molecule (*middle panel*), and the vector normal to a plane of a molecule (*bottom panel*) with the interface normal vector pointing toward the CG region as a function of the x-coordinate in the simulation box. Figure adapted from Zavadlav et al. (2014a)

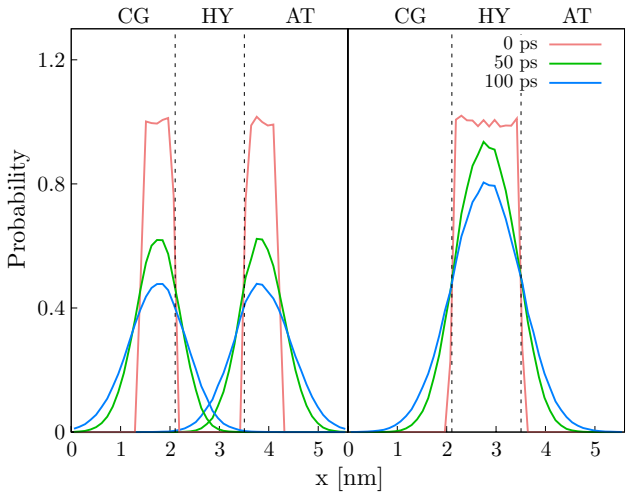

Fig. 5 Diffusion of centers of mass of bundled water molecules. Normalized density distributions of bundles are depicted at three different times. Figure adapted from Zavadlav et al. (2014a)

demonstrates that the bundles can freely move across adaptive resolution regions without experiencing any boundaries.

The bundles are initially in a slab within the AT, CG, or HY region, but diffuse in time throughout the entire simulation box. Particles from the HY region disperse equally to the AT and CG region, because the diffusion coefficients are similar between the two regions (Zavadlav et al. 2014a).

An adaptive resolution simulation of water using the 4-to-1 supramolecular coupling was also carried out by Nagarajan et al. (2013). The authors constrained their AT water model by a harmonic potential, with the LJ parameters left unmodified. In addition, the CG model employed is not compatible with the MARTINI force field (Marrink et al. 2007). Instead, it is parameterized to reproduce the structural properties of the AT model via the effective interactions derived by the iterative Boltzmann inversion.

Polarizable supramolecular water: coupling of rotational degrees of freedom

We proceed by devoting a few words to the extension of supramolecular mapping to polarizable CG models (Zavadlav et al. 2015a). This represents the first AdResS application to solvents with multi-interaction CG sites. An illustration of the simulated system is shown in Fig. 6.

The multiscale character is achieved by splitting the simulation box along the x-coordinate into regions of different resolution. High-resolution bundled-SPC (defined in "Supramolecular water: 4-to-1 molecular mapping") is employed for the central AT region. The AT region is flanked on both ends by the intermediate hybrid (HY) and

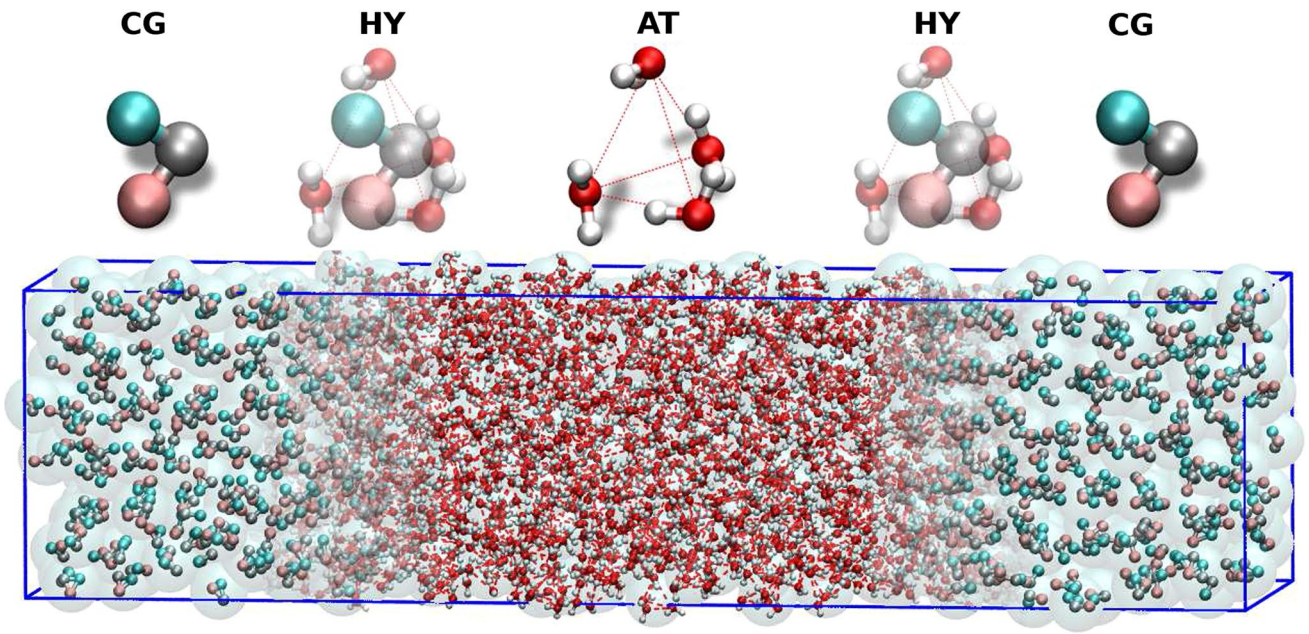

Fig. 6 Schematic representation of the simulated multiscale water system. From the center to the edges of the simulation box, the regions of different resolution change in the horizontal direction from the AT to CG. The corresponding water representation is shown above each region. In the AT region, we use the bundled-SPC model (Fuhrmans et al. 2010), where a water cluster consists of four water molecules that are connected by semi-harmonic springs. The PW (Yesylevskyy et al. 2010) model (consisting of three charged particles) is used in the CG region. The water clusters (shown as *light blue beads*) can change their resolution on the fly as they move through the HY region. Reprinted from Zavadlav et al. (2015a) with the permission of AIP Publishing

subsequently low-resolution CG regions. There we employ the PW (Yesylevskyy et al. 2010) CG water model with explicit charges.

Because the CG representations consist of several interaction sites, we coupled orientational degrees of freedom of the AT and CG representations using a harmonic energy penalty term

$$U_{\alpha}^{\mathrm{rot}} = \frac{1}{2} K \theta_{\alpha}^{2}, \tag{5}$$

where θ_{α} is the angle between the AT and CG dipole moments of a given cluster α. The potential depends on the coordinates of all the AT and CG particles of the cluster, and is therefore able to orient both models so that the two dipoles point in the same direction. At the same time, it leaves the cluster's center of mass intact. In this way, only the direction of the dipole moment is coupled, while the magnitudes still differ. To find the appropriate strength of rotational coupling, we tested several force constants K. The average cosine value of the angle formed by the dipole orientations of the AT and CG representations is depicted in Fig. 7. In the case of no rotational coupling (red and green lines), there is no correlation between the orientations of the AT and CG representations of clusters, whereas drastic improvement is achieved by the incorporation of rotational coupling. In the end, we have set K such that it is moderate, yet sufficient (purple line).

The significance of rotational coupling was further examined by the response of the system to an external static electric field of 1.0 V nm^{-1} applied in the y-direction (Fig. 8).

The average cosine of angle α formed by the dipole and normal vectors pointing toward the CG region as a function of the x-coordinate are presented for two cases: without (left) and with (right) rotational coupling. In both cases we found that, under the external electric field, the clusters' dipole moments aligned with the direction of the field, as opposed to the case without the electric field. The extent of alignment is not the same in all AdResS domains; it is higher in the AT than in the CG region. However, while in both cases the orientation is correctly reproduced in the AT and CG regions, in the HY region fewer artifacts are observed with rotational coupling. In particular, the magnitude of the clusters' alignment is notably improved.

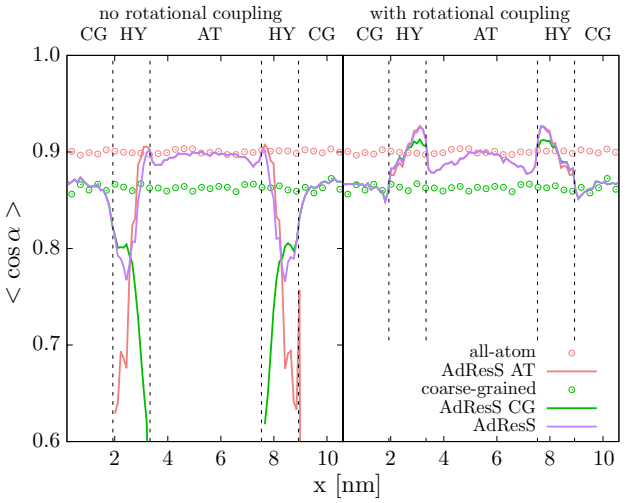

Fig. 8 Properties of a bundled-SPC/PW system subjected to an external electric field. The plots show the average cosine of the angle formed by the dipole vector of the water cluster and vector normal to the boundary and pointing toward the CG region. *Right* and *left panels* show the results with and without rotational coupling, respectively. The results from reference AT and CG simulations are shown as *circles*. Adapted from Zavadlav et al. (2015a) with the permission of AIP Publishing

Multiresolution biomolecular simulations

Multiscale simulations are particularly advantageous for molecular systems where high resolution is required only

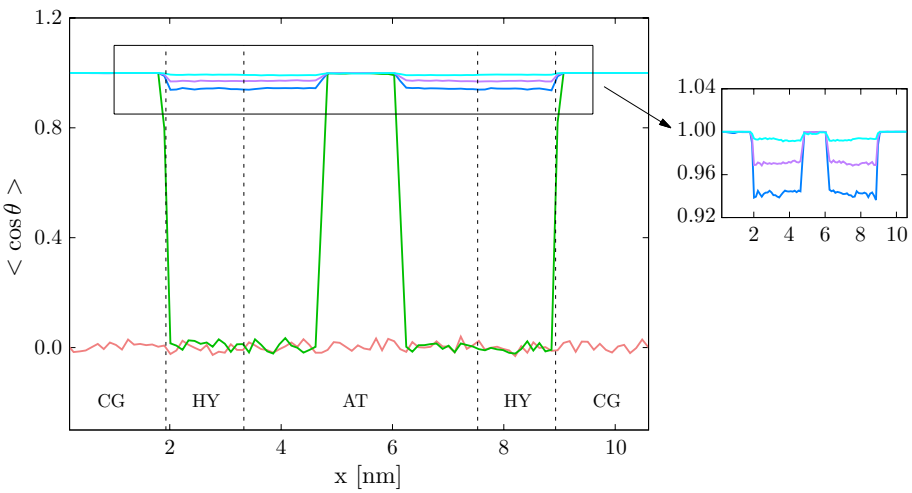

Fig. 7 Average cosine of the angle formed by the AT and CG representation dipole vectors. *Red*, *green*, *blue*, *purple*, and *cyan lines* correspond to increased strength of the rotational coupling (from 0 to 500 kJ mol^{-1} rad^{-2}). Adapted from Zavadlav et al. (2015a) with the permission of AIP Publishing

in spatially localized domains, and a lower resolution is sufficient for the rest of the system, as in the case of biophysical macromolecules. This has led to the development of hybrid schemes—see, for example, Rzepiela et al. (2011), Shi et al. (2006), Masella et al. (2008, 2011), Riniker et al. (2012a), Michel et al. (2008), Gonzales et al. (2013), Han and Schulten (2012), Neri et al. (2005), and Alekseevaa et al. (2016)—but in almost all cases, the resolution of molecules is kept fixed during the simulation. Problems may arise when such schemes are applied to macromolecules in multiscale solutions. Typically, the fine-grained water molecules have to be restrained to the vicinity of the protein's surface to prevent them from drifting away from the protein (Riniker et al. 2012b; Sokkar et al. 2013, 2015). Such non-physical restrictions then lead to artifacts, such as too high density of the AT solvent (Kuhn et al. 2015). These undesirable outcomes can be avoided by AdResS, which allows molecules to change their resolution on the fly.

Atomistic protein in MARTINI water: stability of solvated macromolecule

As the first application of the AdResS scheme to biological macromolecules, we simulated a fully AT protein G solvated in a multiresolution water (see "Supramolecular water: 4-to-1 molecular mapping") at ambient conditions (Zavadlav et al. 2014b). The system is schematically illustrated in Fig. 9.

Protein G was selected as it is well-studied and has a secondary structure that contains an α-helix as well as a β-sheet. The solvent's level of representation depends on the distance from the protein's center of mass. For short distances, we resort to the bundled-SPC model to properly incorporate the specific hydrogen-bonding pattern. For the description of the water farther away, where high resolution is not required, we use the mesoscopic MARTINI CG model. As discussed in "Supramolecular water: 4-to-1 molecular mapping", by using the bundled-SPC water as our AT water model, we avoid theoretical difficulties of both the AdResS and the coarse-graining of several non-bonded particles (e.g., solvent molecules) into one CG bead, that arise when the AT molecules can drift apart.

The AdResS approach for the present protein–water system was tested via analysis of the structural and dynamic properties of a protein in the multiscale solvent. We investigated three sizes of the AT sphere radius to gain insight into the extent of the influence of the bulk on the local hydrogen bond network in the hydration shell. The multiscale results are compared to the corresponding fully AT system where all water molecules are modeled with a high level of detail, i.e., either with the bundled-SPC or the SPC model (Zavadlav et al. 2014b). The atom-positional root-mean-square deviation (RMSD) and fluctuation (RMSF) are used for quantitative assessment of how well a simulated structure matches the reference state.

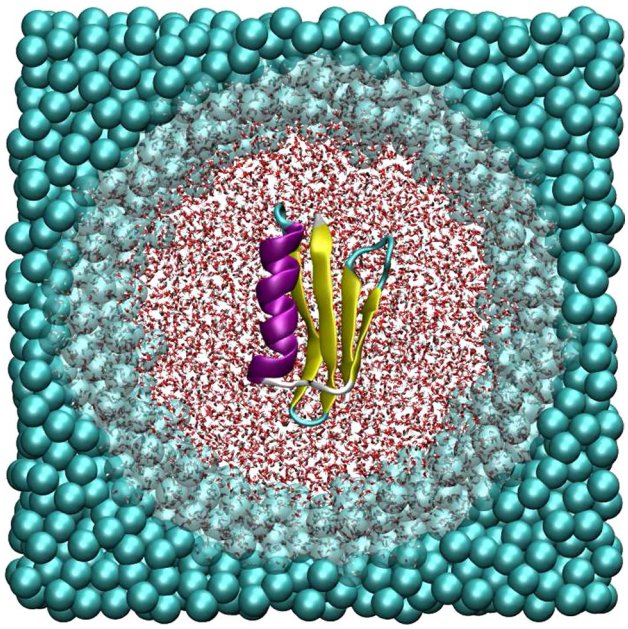

Fig. 9 A schematic cross section of simulation box with spherical adaptive resolution regions. Two levels of resolution are used for solvent molecules. A high level of resolution (bundled-SPC water model) is used for solvent molecules within a certain radius from the protein's center of mass. A low level of resolution (MARTINI) is used for solvent molecules elsewhere. The protein G is thus fully AT at all times, but is shown here in cartoon representation for better clarity. Figure reprinted from Zavadlav et al. (2014b)

In our case, the two properties are used to show that the multiscale simulation does not affect the structural properties of the protein. The results plotted in Fig. 10 reveal that the structure of the protein is stable in all simulations considered. The values obtained are in agreement with previously published results (Riniker et al. 2012b) and with the reference fully AT simulations.

The dynamic properties of the protein and solvent are also in agreement with the fully AT results. The diffusion coefficient for the protein is an order of magnitude smaller than that for bundled water (Zavadlav et al. 2014b). This result also justifies our simulation setup of moving the center of the AT resolution region along with the protein's center of mass. The slower movement of the protein is essential, as it enables the solvent molecules to adequately equilibrate their degrees of freedom upon crossing the borders of domains with a different resolution.

Fogarty et al. (2015) recently conducted an AdResS simulation of a protein ubiquitin in multiscale water with 1-to-1 molecular mapping. Their conclusions are in accord with our findings for the protein G, that AdResS simulations faithfully reproduce reference all-atom results.

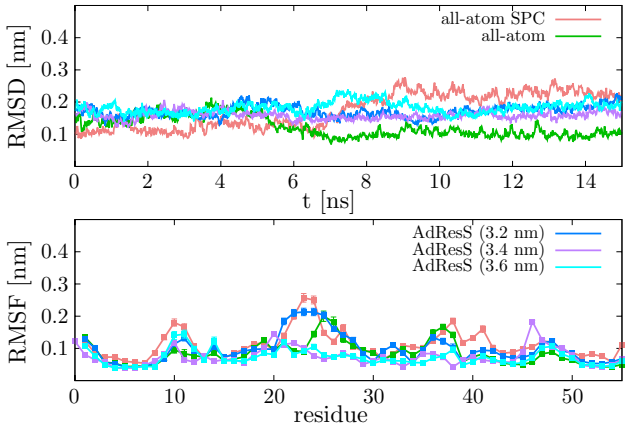

Fig. 10 Root-mean-square deviation (RMSD, *top*) and fluctuation (RMSF) with *error bars* (*bottom*) of the backbone non-hydrogen atoms with respect to the initial crystal structure (PDB entry 1PGB). We compare the results obtained from the simulation with SPC and bundled-SPC solvations for three spherical AT region sizes of 3.2, 3.4, and 3.6 nm. Figure adapted from Zavadlav et al. (2014b)

Atomistic DNA molecule in salt solution: dielectric properties

The structure and stability of a DNA molecule is strongly dependent on the environment, i.e., the surrounding ions and water. A DNA molecule, in turn, strongly influences the surrounding aqueous solvent. As a consequence, the solvent's properties within the first two coordination shells from the DNA molecule deviate substantially from bulk values (Stanley and Rau 2011). For example, water is found to be considerably ordered and has slower dynamics due to the motional restrictions imposed by the DNA and the ions (Bagchi 2012). Together, these features give rise to a very complicated, spatially varying dielectric permittivity of both DNA and the surrounding solvent (Gavryushov 2008; Lamm and Pack 1997; Young et al. 1998). The dielectric permittivity of biological macromolecules is very difficult to determine experimentally, and the dielectric permittivity of DNA has only recently been measured successfully (Cuervo et al. 2014). All-atom MD simulations of these systems are also computationally challenging, because the natural DNA environment is a salt solution. For statistical reasons, this requires a significant number of ions and, consequently, large simulation systems. Although the CG models (Potoyan et al. 2013; Snodin et al. 2015; Maciejczyk et al. 2014; Knotts et al. 2007) are continually being improved, they are still not adequate for describing the spatially varying dielectric environments. Thus, multiscale methods such as the AdResS offer a promising approach for tackling this type of problem.

Here, we briefly describe a multiscale simulation of a double-stranded 10-base-pair DNA molecule in a 1 M NaCl electrolyte bath by employing a hybrid AT/CG solvent model discussed in "Salt solution: 1-to-1 molecular mapping". A schematic representation of the simulated system is depicted in Fig. 11.

We have employed PBCs along the DNA helix where patches—i.e., corresponding intramolecular DNA interactions defined by bond, angle, and dihedral interaction potentials—are used to connect each strand to its periodic image along the z-axis. This simulation setup enables us to mimic an infinitely long DNA molecule, and is better suited for comparison with experimental studies where the DNA molecules are commonly ordered and densely packed (Korolev et al. 2006).

As already mentioned, special attention has been given to the calculation of dielectric permittivity, as it provides a sensitive quality measure of our multiscale approach. To compute the dielectric permittivity of water around the DNA molecule, we employ Kirkwood's theory, where the dielectric permittivity is related to the average vector sum of the dipole moments of the individual water molecules in a

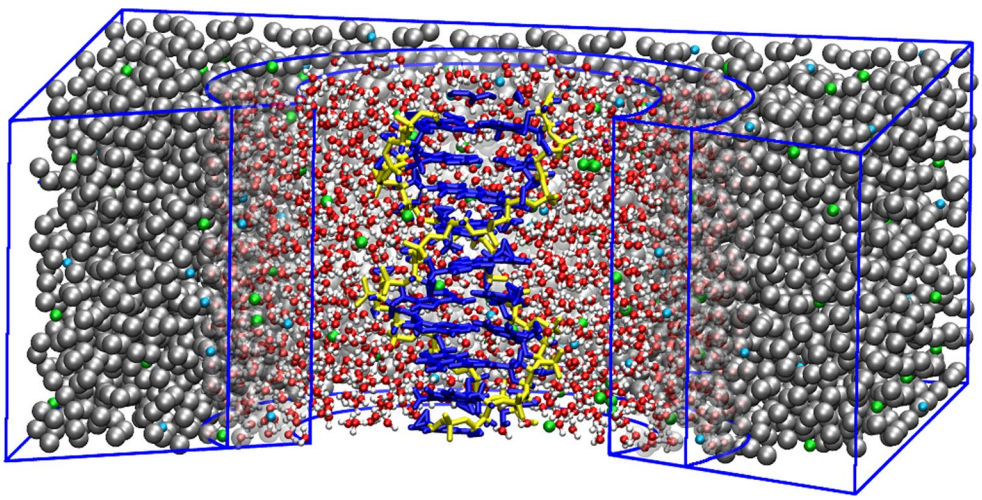

Fig. 11 Schematic cross section of simulation box with cylindrical resolution regions. Two levels of resolution are used for solvent molecules. A high level of resolution is used for solvent molecules within a certain radius from the DNA's center of mass. The water molecules farther away are represented as single beads (*gray*). The Na^+ and Cl^- ions are shown in *green* and *blue*, respectively. Reprinted with permission from Zavadlav et al. (2015b). Copyright 2015 American Chemical Society

spherical region (Young et al. 1998; Zavadlav et al. 2015b). Figure 12 shows the dielectric profile of water in the AT and HY regions around the DNA molecule.

The dielectric permittivity increases with distance from the DNA's center of mass and reaches the bulk value around 1.7 nm. As expected, the bulk dielectric permittivity is smaller than the value for pure water (82 for TIP3P water model), because the movement of water is restricted by the ions. In all AdResS simulations, the dielectric permittivity decreases in the HY region. The water molecules in the CG region are chargeless particles. Therefore, as they move from the AT to the HY region, the AT interactions are gradually switched off, and the molecules lose their rotational degrees of freedom. As a result of this rotational freezing, the dielectric permittivity is lower. We also observe a rise in the dielectric permittivity at the AT/HY transition. Note that there is a slight orientational order, since the average cosine value of the angle formed by the water's dipole moment and the normal vector pointing toward the CG region is not equal to zero (similar to what is seen in Fig. 4). Figure 12 also points out the necessary size of the AT region. If, for example, the goal of the multiscale simulation is to reproduce the behavior of the fully AT system in the first two hydration shells, the radius of the AT region must be at least 1.8 nm. For further results on dielectric permittivity, we refer the reader to Zavadlav et al. (2015b).

Computational speedup

One of the objectives of multiscale MD simulations is to reduce the huge computational resources required in conventional monoscale simulations. A theoretical route for the estimation of multiscale speedup is to consider the most cumbersome part of MD simulation, i.e., the evaluation of the non-bonded interactions. In an N-atom system, the non-bonded contribution to the forces requires, in principle, $N(N-1)/2$ calculations. If the total system is instead modeled at the CG resolution, the complexity is reduced considerably. For example, in the case of the MARTINI water model where four water molecules (consisting of three atoms) are replaced by a single particle, the number of pairwise calculations is reduced to $N(N-12)/(144\times 2)$ (replacing N with $N/12$ in the previous equation). For the polarizable CG water models, the corresponding value is $N(N-4)/(16\times 2)$. For the CG water models, in which a CG bead represents a single water molecule, the reduction in complexity is much less $N(N-3)/(9\times 2)$. However, such estimations serve only as a theoretical limit, since in practice, the number of pairwise calculations is smaller due to grid subdivision of the system and potential cutoffs (Allen and Tildesley 1989), and thus speedup also depends on the models used.

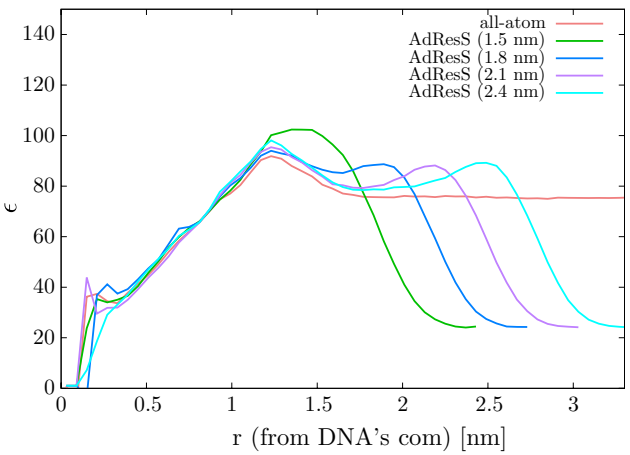

Fig. 12 Calculated dielectric permittivity of water around DNA shown as a function of distance from DNA's center of mass. The results are shown for the AdResS simulations with various AT region sizes and compared to all-atom solvation. Adapted with permission from Zavadlav et al. (2015b). Copyright 2015 American Chemical Society

In the AdResS simulations, the system is represented only in part on the CG level. Compared to the fully AT simulation, the actual speedup therefore depends on the ratio between the AT and CG domain sizes. In addition, the total speedup of the simulation will also depend on the hardware and the code optimization for the selected method and hardware. Our simulation studies are performed with the ESPResSo++ code (Halverson et al. 2013) on a CROW (Crow 0000) Linux cluster. The observed enhancements are approximately one order of magnitude. An analysis of the ESPResSo++ code can be found in Halverson et al. (2013) and Bevc (2013). The code has been tested, for example, on tetrahedral molecules, where it was found that when the whole box in AdResS was set to the CG resolution, the simulation time was half that when the whole region was set to AT resolution, while the multiscale simulations fell in between (Bevc 2013).

The incorporation of a CG domain reduces the computational cost both in terms of reduced degrees of freedom, and potentially in terms of softer interactions. For example, the MARTINI force field can be used with an integration time step of 25 fs (Periole and Marrink 2013), while the usual time step for the AT simulations is 1 fs. The speedup could thus be even greater if the system is tackled on multiple time scales, i.e., with the implementation of a multiple time-scale integration algorithm (Tuckerman 2010).

The computational enhancement is important, because the hydrodynamic interactions are long-range in nature, and large systems are needed to avoid finite size effects. Our supramolecular approach falls between the multiresolution approaches with concurrent coupling of AT water to a CG water (Praprotnik et al. 2008), where one bead represents

one water molecule, and hybrid methods interfacing AT description with continuum (e.g., Walther et al. 2012; Delgado-Buscalioni et al. 2009). Hence, it bridges the hydrodynamics from the atomic to mesoscopic scale and enables the study of biophysical phenomena that are beyond the scope of either AT or mesoscopic simulations (Zavadlav 2015).

Conclusions

This contribution presents a review of recent adaptive resolution approaches to biomolecular systems. The focus is on the AdResS method for the coupling of atomistic and coarse-grained solvent models to solvate biomacromolecules. In the examples presented, the biomacromolecules and the proximal solvent are modeled fully atomistically, whereas the distal solvent is represented using a coarse-grained model. Specifically, we discuss two different coarse-graining mappings, the 1-to-1 and 4-to-1 molecular mappings. The latter is necessary if one wants to couple atomistic solvent with the widely used MARTINI force field. To this end, one must resort to the bundled atomistic water models, where four given water molecules are connected with additional semi-harmonic bonds in order to ensure a feasible multimolecular coupling.

The performance of the bundled water compared to the unrestrained SPC model was critically evaluated previously in Fuhrmans et al. (2010), Gopal et al. (2015), Zavadlav et al. (2014b, 2016b), and Nagarajan et al. (2013). The largest discrepancies were found in the properties of the water itself, while as a solvent, the bundled model in most cases performed quite well. For example, comparable results were found for the thermodynamic behavior of amino acid residues and conformational analysis of short peptides. Similarly, our adaptive resolution simulations of protein solvation show no notable difference in the protein structural analysis between the bundled-SPC and SPC solvations. However, in some cases, bundling may lead to substantial artifacts, such as partial unfolding of the coiled-coil dimer (Gopal et al. 2015).

To overcome these deficiencies, our current efforts are directed toward a supramolecular coupling, where bundled atomistic water models are no longer required (Zavadlav et al. 2016a).

Acknowledgements We would like to thank S. J. Marrink and M. N. Melo for a fruitful collaboration on coupling atomistic and MARTINI molecular models for biomolecular simulations. We are grateful to C. Junghans and K. Kremer for collaboration on the salt solution. We would also like to thank R. Podgornik for collaborating with us on the DNA simulations and J. Sablić for careful reading of the manuscript. We acknowledge financial support through grants P1-0002 and J1-7135 from the Slovenian Research Agency.

References

Agarwal A, Delle Site L (2015) Path integral molecular dynamics within the grand canonical-like adaptive resolution technique: simulation of liquid water. J Chem Phys 143:094102

Agarwal A, Delle Site L (2016) Grand-canonical adaptive resolution centroid molecular dynamics: Implementation and application. Comput Phys Commun 206:26–34

Agarwal A, Wang H, Schütte C, Delle Site L (2014) Chemical potential of liquids and mixtures via adaptive resolution simulation. J. Chem. Phys. 141:034102

Alekseevaa U, Winklerc RG, Sutmanna G (2016) Hydrodynamics in adaptive resolution particle simulations: multiparticle collision dynamics. J Comput Phys 314:14–34

Allen MP, Tildesley DJ (1989) Computer simulation of liquids. Oxford University Press, New York

Ayton GS, Noid WG, Voth GA (2007) Multiscale modeling of biomolecular systems: in serial and in parallel. Curr Opin Struct Biol 17:192–198

Bagchi B (2012) From anomalies in neat liquid to structure, dynamics and function in the biological world. Chem Phys Lett 529:1–9

Basdevant N, Borgis D, Ha-Duong T (2007) A coarse-grained protein–protein potential derived from an all-atom force field. J Phys Chem B 111:9390–9399

Bereau T, Deserno M (2009) Generic coarse-grained model for protein folding and aggregation. J Chem Phys 130:235106

Bevc S (2013) Razvoj računalniških orodij za molekularno modeliranje. PhD thesis, Faculty of Mathematics, Natural Sciences and Information Technologies, University of Primorska

Bevc S, Junghans C, Kremer K, Praprotnik M (2013) Adaptive resolution simulation of salt solutions. New J Phys 15:105007

Bevc S, Junghans C, Praprotnik M (2015) Stock: structure mapper and online coarse-graining kit for molecular simulations. J Comput Chem 36:467–477

Bock H, Gubbins KE, Klapp SH (2007) Coarse graining of nonbonded degrees of freedom. Phys Rev Lett 98:267801

Cameron A (2005) Concurrent dual-resolution Monte Carlo simulation of liquid methane. J Chem Phys 123:234101

Carmichael SP, Shell MS (2012) A new multiscale algorithm and its application to coarse-grained peptide models for self-assembly. J Phys Chem B 116:8383–8393

Crow = Columns and Rows of Workstations. http://www.cmm.ki.si/vrana/. 28 August 2015

Chebaro Y, Pasquali S, Derreumaux P (2012) The coarse-grained OPEP force field for non-amyloid and amyloid proteins. J Phys Chem B 116:8741–8752

Chopraa G, Summab CM, Levitt M (2008) Solvent dramatically affects protein structure refinement. Proc Natl Acad Sci USA 105:20239–20244

Cragnolini T, Derreumaux P, Pasquali S (2013) Coarse-grained simulations of RNA and DNA duplexes. J Phys Chem B 117:8047–8060

Cuervo A, Dans PD, Carrascosa JL, Orozco M, Gomila G, Fumagalli L (2014) Direct measurement of the dielectric polarization properties of DNA. Proc Natl Acad Sci USA 111:3624–3630

Dans PD, Walther J, Gómez H, Orozco M (2016) Multiscale simulation of DNA. Curr Opin Chem Biol 37:29–45

Dans PD, Zeida A, Machado MR, Pantano S (2010) A coarse grained model for atomic-detailed DNA simulations with explicit electrostatics. J Chem Theory Comput 6:1711–1725

Delgado-Buscalioni R, Kremer K, Praprotnik M (2008) Concurrent triple-scale simulation of molecular liquids. J Chem Phys 128:114110

Delgado-Buscalioni R, Kremer K, Praprotnik M (2009) Coupling atomistic and continuum hydrodynamics through a mesoscopic model: application to liquid water. J Chem Phys 131:244107

Delgado-Buscalioni R, Sablić J, Praprotnik M (2015) Open boundary molecular dynamics. Eur Phys J Spec Top 224:2331–2349

Delgado-Buscalioni R, Sablić J, Praprotnik M (2015) Reply to comment by R. Klein on open boundary molecular dynamics. Eur Phys J Spec Top 224:2511–2513

Delle Site L (2016) Formulation of Liouville's theorem for grand ensemble molecular simulations. Phys Rev E 93:022130

Delle Site L, Abrams CF, Alavi A, Kremer K (2002) Polymers near metal surfaces: selective adsorption and global conformations. Phys Rev Lett 89:156103

Duan Y, Wu C, Chowdhury S, Lee M, Xiong G, Zhang W, Yang R, Cieplak P, Luo R, Lee T, Caldwell J, Wang J, Kollman P (2003) A point-charge force field for molecular mechanics simulations of proteins based on condensed-phase quantum mechanical calculations. J Comput Chem 24:1999–2012

Español P, Delgado-Buscalioni R, Everaers R, Potestio R, Donadio D, Kremer K (2015) Statistical mechanics of Hamiltonian adaptive resolution simulations. J Chem Phys 142:064115

Fabritiis GD, Delgado-Buscalioni R, Coveney PV (2006) Multiscale modeling of liquids with molecular specificity. Phys Rev Lett 97:134501

Fedosov DA, Karniadakis GE (2009) Triple-decker: interfacing atomistic–mesoscopic–continuum flow regimes. J Comput Phys 228:1157–1171

Fogarty AC, Potestio R, Kremer K (2015) Adaptive resolution simulation of a biomolecule and its hydration shell: structural and dynamical properties. J Chem Phys 142:195101

Fogarty AC, Potestio R, Kremer K (2016) A multi-resolution model to capture both global fluctuations of an enzyme and molecular recognition in the ligand-binding site. Proteins Struct Funct Bioinform 84:1902–1913

Foley T, Shell MS, Noid WG (2015) The impact of resolution upon entropy and information in coarse-grained models. J Chem Phys 143:243104

Frenkel D, Smit B (2001) Understanding molecular simulation: from algorithms to applications. Academic Press, San Diego

Fritsch S, Poblete S, Junghans C, Ciccotti G, Delle Site L, Kremer K (2012) Adaptive resolution molecular dynamics simulation through coupling to an internal particle reservoir. Phys Rev Lett 108:170602

Fuhrmans M, Sanders BP, Marrink SJ, de Vries AH (2010) Effects of bundling on the properties of the SPC water model. Theor Chem Acc 125:335–344

Gavryushov S (2008) Electrostatics of B-DNA in NaCl and $CaCl_2$ solutions: ion size, interionic correlation, and solvent dielectric saturation effects. J Phys Chem B 112:8955–8965

Goga N, Costache S, Marrink SJ (2009) A multiscalling constant lambda molecular dynamic gromacs implementation. Mater Plast 46:53–57

Gonzales HC, Darré L, Pantano S (2013) Transferable mixing of atomistic and coarse-grain water models. J Phys Chem B 117:14438–14448

Gopal S, Mukherjee S, Cheng YM, Feig M (2010) PRIMO/PRIMONA: a coarse-grained model for proteins and nucleic acids that preserves near-atomistic accuracy. Proteins Struct Funct Bioinform 78:1266–1281

Gopal SM, Kuhn AB, Schäfer LV (2015) Systematic evaluation of bundled SPC water for biomolecular simulations. Phys Chem Chem Phys 17:8393–8406

Halverson JD, Brandes T, Lenz O, Arnold A, Bevc S, Starchenko V, Kremer K, Stuehn T, Reith D (2013) ESPResSo++: a modern multiscale simulation package for soft matter systems. Comput Phys Commun 184:1129–1149

Han W, Schulten K (2012) Further optimization of a hybrid united-atom and coarse-grained force field for folding simulations: improved backbone hydration and interactions between charged side chains. J Chem Theory Comput 8:4413–4424

Harmandarisab VA, Adhikari NP, van der Vegt NFA, Kremer K (2006) Hierarchical modeling of polystyrene: from atomistic to coarse-grained simulations. Macromolecules 39:67086719

Harmandarisab VA, Kremer K (2009) Predicting polymer dynamics at multiple length and time scales. Soft Matter 5:3920–3926

Hess B, León S, van der Vegt N, Kremer K (2006) Long time atomistic polymer trajectories from coarse grained simulations: bisphenol-A polycarbonate. Soft Matter 2:409–414

Heyden A, Truhlar DG (2008) Conservative algorithm for an adaptive change of resolution in mixed atomistic/coarse-grained multiscale simulations. J Chem Theory Comput 4:217–221

Hinckley DM, Lequieu JP, de Pablo JJ (2014) Coarse-grained modeling of DNA oligomer hybridization: length, sequence, and salt effects. J Chem Phys 141:035102

Ingólfsson HI, Lopez CA, Uusitalo JJ, de Jong DH, Gopal S, Periole X, Marrink SJ (2014) The power of coarse-graining in biomolecular simulations. WIREs Comput Mol Sci 4:225–248

Izvekov S, Parrinello M, Burnham CB, Voth GA (2004) Effective force fields for condensed phase systems from ab initio molecular dynamics simulation: a new method for force-matching. J Chem Phys 120:10896–10913

Izvekov S, Voth GA (2005) A multiscale coarse-graining method for biomolecular systems. J Phys Chem B 109:2469–2473

Izvekov S, Voth GA (2005) Multiscale coarse graining of liquid-state systems. J Chem Phys 123:134105

Izvekov S, Voth GA (2006) Multiscale coarse-graining of mixed phospholipid/cholesterol bilayers. J Chem Theory Comput 2:637648

Jedlovszky P, Vincze A, Horvai G (2007) Full description of the orientational statistics of molecules near to interfaces. Water at the interface with CCl4. Phys Chem Chem Phys 6:1874–1879

Jorgensen WL, Chandrasekhar J, Madura JD, Impey RW, Klein ML (1983) Comparison of simple potential functions for simulating liquid water. J Chem Phys 79:926–935

Kamerlin SCL, Vicatos S, Dryga A, Warshel A (2011) Coarse-grained (multiscale) simulations in studies of biophysical and chemical systems. Annu Rev Phys Chem 62:41–64

Karplus M, McCammon JA (2002) Molecular dynamics simulations of biomolecules. Nat Struct Biol 9:646–652

Knotts TAI, Rathore N, Schwartz DC, de Pablo JJ (2007) A coarse grain model for DNA. J Chem Phys 126:084901

Korolev N, Lyubartsev AP, Laaksonen A, Nordenskiöld L (2006) A molecular dynamics simulation study of oriented DNA with polyamine and sodium counterions: diffusion and averaged binding of water and cations. Nucleic Acids Res 31:5971–5981

Kranenburg M, Nicolas JP, Smit B (2004) Comparison of mesoscopic phospholipid–water models. Phys Chem Chem Phys 6:4142–4151

Kreis K, Donadio D, Kremer K, Potestio R (2014) A unified framework for force-based and energy-based adaptive resolution simulations. EPL 108:30007

Kreis K, Fogarty A, Kremer K, Potestio R (2015) Advantages and challenges in coupling an ideal gas to atomistic models in adaptive resolution simulations. Eur Phys J Spec Top 224:2289–2304

Kreis K, Potestio R, Kremer K, Fogarty AC (2016) Adaptive resolution simulations with self-adjusting high-resolution regions. J Chem Theory Comput 12:4067–4081

Kuhn AB, Gopal SM, Schäfer LV (2015) On using atomistic solvent layers in hybrid all-atom/coarse-grained molecular dynamics simulations. J Chem Theory Comput 11:4460–4472

Lamm G, Pack GR (1997) Calculation of dielectric constants near polyelectrolytes in solution. J Phys Chem B 101:959–965

Lu J, Yuqing Qiu Y, Baron R, Molinero V (2014) Coarse-graining of TIP4P/2005, TIP4P-Ew, SPC/E, and TIP3P to monatomic

anisotropic water models using relative entropy minimization. J Chem Theory Comput 10:4104–4120
Lyubartsev AP (2005) Multiscale modeling of lipids and lipid bilayers. Eur Biophys J 35:53–61
Lyubartsev AP, Laaksonen A (1995) Calculation of effective interaction potentials from radial distribution functions: a reverse Monte Carlo approach. Phys Rev E 52:3730–3737
Lyubartsev AP, Naômé A, Vercauteren DP, Laaksonen A (2015) Systematic hierarchical coarse-graining with the inverse Monte Carlo method. J Chem Phys 143:243120
Machado MR, Dans PD, Pantano S (2011) A hybrid all-atom/coarse grain model for multiscale simulations of DNA. Phys Chem Chem Phys 13:18134–18144
Machado MR, Pantano S (2015) Exploring LacI–DNA dynamics by multiscale simulations using the SIRAH force field. J Chem Theory Comput 11:5012–5023
Maciejczyk M, Spasic A, Liwo A, Scheraga HA (2014) DNA duplex formation with a coarse-grained model. J Chem Theory Comput 10:5020–5035
Maffeo C, Ngo TTM, Ha T, Aksimentiev A (2014) A coarse-grained model of unstructured single-stranded DNA derived from atomistic simulation and single-molecule experiment. J Chem Theory Comput 10:2891–2896
Marrink SJ, Risselada HJ, Yefimov S, Tieleman DP, de Vries AH (2007) The martini force field: coarse grained model for biomolecular simulations. J Phys Chem B 111:7812–7824
Masella M, Borgis D, Cuniasse P (2008) Combining a polarizable force-field and a coarse-grained polarizable solvent model: application to long dynamics simulations of bovine pancreatic trypsin inhibitor. J Comput Chem 29:1707–1724
Masella M, Borgis D, Cuniasse P (2011) Combining a polarizable force-field and a coarse-grained polarizable solvent model. II. Accounting for hydrophobic effects. J Comput Chem 32:2664–2678
Matysiak S, Clementi C, Praprotnik M, Kremer K, Delle Site L (2008) Modeling diffusive dynamics in adaptive resolution simulation of liquid water. J Chem Phys 128:024503
Michel J, Orsi M, Essex JW (2008) Prediction of partition coefficients by multiscale hybrid atomic-level/coarse-grain simulations. J Phys Chem B 112:657–660
Mohamed KM, Mohamad AA (2010) A review of the development of hybrid atomistic-continuum methods for dense fluids. Microfluid Nanofluid 8:283–302
Monticelli L, Kandasamy SK, Periole X, Larson RG, Tieleman DP, Marrink SJ (2008) The MARTINI coarse grained force field: extension to proteins. J Chem Theory Comput 4:819–834
Mukherji D, Kremer K (2013) Coil–globule–coil transition of pnipam in aqueous methanol: coupling all-atom simulations to semi-grand canonical coarse-grained reservoir. Macromolecules 46:9158–9163
Mullinax JW, Noid WG (2009) Extended ensemble approach for deriving transferable coarse-grained potentials. J Chem Phys 131:104110
Nagarajan A, Junghans C, Matysiak S (2013) Multiscale simulation of liquid water using a four-to-one mapping for coarse-graining. J Chem Theory Comput 9:5168–5175
Neri M, Anselmi C, Cascella M, Maritan A, Carloni P (2005) Coarse-grained model of proteins incorporating atomistic detail of the active site. Phys Rev Lett 95:218102
Neumann M (1983) Dipole-moment fluctuation formulas in computer-simulations of polar systems. Mol Phys 50:841–858
Neumann M (1985) The dielectric constant of water. Computer simulations with the MCY potential. J Chem Phys 82:5663–5672
Nielsen SO, Moore PB, Ensing B (2010) Adaptive multiscale molecular dynamics of macromolecular fluids. Phys Rev Lett 105:237802
Noid WG (2013) Perspective: Coarse-grained models for biomolecular systems. J Chem Phys 139:090901
Orsi M, Ding W, Palaiokostas M (2014) Direct mixing of atomistic solutes and coarse-grained water. J Chem Theory Comput 10:4684–4693
Orsi M, Essex JW (2011) The ELBA force field for coarse-grain modeling of lipid membranes. PLoS One 6:e28637
Ouldridge TE, Louis AA, Doye JPK (2011) Structural, mechanical and thermodynamic properties of a coarse-grained DNA model. J Chem Phys 134:085101
Periole X, Marrink SJ (2013) The MARTINI coarse-grained force field. In: Monticelli L, Salonen E (eds) Biomolecular simulations: methods and protocols, methods in molecular biology, vol 924. Springer, New York, pp 533–565
Peter C, Kremer K (2009) Multiscale simulation of soft matter systems—from the atomistic to the coarse-grained level and back. Soft Matter 5:4357–4366
Peters JH, Klein R, Delle Site L (2016) Simulation of macromolecular liquids with the adaptive resolution molecular dynamics technique. Phys Rev E 94:023309
Poblete S, Praprotnik M, Kremer K, Delle Site L (2010) Coupling different levels of resolution in molecular simulations. J Chem Phys 132:114101
Poma AB, Delle Site L (2010) Classical to path-integral adaptive resolution in molecular simulation: towards a smooth quantum-classical coupling. Phys Rev Lett 104:250201
Poma AB, Delle Site L (2011) Adaptive resolution simulation of liquid para-hydrogen: testing the robustness of the quantum-classical adaptive coupling. Phys Chem Chem Phys 13:10510–10519
Potestio R, Español P, Delgado-Buscalioni R, Everaers R, Kremer K, Donadio D (2013) Monte Carlo adaptive resolution simulation of multicomponent molecular liquids. Phys Rev Lett 111:060601
Potestio R, Fritsch S, Español P, Delgado-Buscalioni R, Kremer K, Everaers R, Donadio D (2013) Hamiltonian adaptive resolution simulation for molecular liquids. Phys Rev Lett 110:108301
Potestio R, Peter C, Kremer K (2014) Computer simulations of soft matter: linking the scales. Entropy 16:4199–4245
Potoyan DA, Savelyev A, Papoian GA (2013) Recent successes in coarse-grained modeling of DNA. WIREs Comput Mol Sci 3:69–83
Praprotnik M, Delle Site L, Kremer K (2005) Adaptive resolution molecular-dynamics simulation: changing the degrees of freedom on the fly. J Chem Phys 123:224106
Praprotnik M, Delle Site L, Kremer K (2008) Multiscale simulation of soft matter: from scale bridging to adaptive resolution. Annu Rev Phys Chem 59:545–571
Praprotnik M, Matysiak S, Delle Site L, Kremer K, Clementi C (2007) Adaptive resolution simulation of liquid water. J Phys Condens Matter 19:292201
Praprotnik M, Poblete S, Kremer K (2011) Statistical physics problems in adaptive resolution computer simulations of complex fluids. J Stat Phys 145:946–966
Reith D, Pütz M, Müller-Plathe F (2003) Deriving effective mesoscale potentials from atomistic simulations. J Comput Chem 24:1624–1636
Reynwar BJ, Illya G, Harmandaris VA, Müller MM, Kremer K, Deserno M (2007) Aggregation and vesiculation of membrane proteins by curvature-mediated interactions. Nature 447:461
Riniker S, Eichenberger AP, van Gunsteren WF (2012) Solvating atomic level fine-grained proteins in supra-molecular level coarse-grained water for molecular dynamics simulations. Eur Biophys J 41:647–661
Riniker S, Eichenberger AP, van Gunsteren WF (2012) Structural effects of an atomic-level layer of water molecules around proteins solvated in supra-molecular coarse-grained water. J Phys Chem B 116:8873–8879

Riniker S, van Gunsteren WF (2011) A simple, efficient polarizable coarse-grained water model for molecular dynamics simulations. J Chem Phys 134:084110

Rudzinski JF, Noid WG (2015) Bottom–up coarse-graining of peptide ensembles and helixcoil transitions. J Chem Theory Comput 11:1278–1291

Rzepiela AJ, Louhivuori M, Peter C, Marrink SJ (2011) Hybrid simulations: combining atomistic and coarse-grained force fields using virtual sites. Phys Chem Chem Phys 13:10437–10448

Sablić J, Praprotnik M, Delgado-Buscalioni R (2016) Open boundary molecular dynamics of sheared star-polymer melts. Soft Matter 12:2416–2439

Savelyev A, Papoian GA (2010) Chemically accurate coarse graining of double-stranded DNA. Proc Natl Acad Sci USA 107:20340–20345

Shaw DE, Deneroff MM, Dror RO, Kuskin JS, Larson RH, Salmon JK, Young C, Batson B, Bowers KJ, Chao JC, Eastwood MP, Gagliardo J, Grossman JP, Ho CR, Ierardi DJ, Kolossváry I, Klepeis JL, Layman T, McLeavey C, Moraes MA, Mueller R, Priest EC, Shan Y, Spengler J, Theobald M, Towles B, Wang SC (2007) Anton, a special-purpose machine for molecular dynamics simulation. SIGARCH Comput Archit News 35:1–12

Shell MS (2008) The relative entropy is fundamental to thermodynamic ensemble optimization. J Chem Phys 129:144108

Shelley JC, Shelley MY, Reeder R, Bandyopadhyay S, Klein ML (2001) A coarse grained model for phospholipid simulations. J Phys Chem B 105:4464–4470

Shen L, Hu H (2014) Resolution-adapted all-atomic and coarse-grained model for biomolecular simulations. J Chem Theory Comput 10:2528–2536

Shen L, Yang W (2016) Quantum mechanics/molecular mechanics method combined with hybrid all-atom and coarse-grained model: Theory and application on Redox potential calculations. J Chem Theory Comput. doi:10.1021/acs.jctc.5b01107

Shi Q, Izvekov S, Voth GA (2006) Mixed atomistic and coarse-grained molecular dynamics: simulation of a membrane-bound ion channel. J Phys Chem B 110:15045–15048

Snodin BEK, Randisi F, Mosayebi M, Sulc P, Schreck JS, Romano F, Ouldridge TE, Tsukanov R, Nir E, Louis AA, Doye JPK (2015) Introducing improved structural properties and salt dependence into a coarse-grained model of DNA. J Chem Phys 142:234901

Sokkar P, Boulanger E, Thiel W, Sanchez-Garcia E (2015) Hybrid quantum mechanics/molecular mechanics/coarse grained modeling: a triple-resolution approach for biomolecular systems. J Chem Theory Comput 11:1809–1818

Sokkar P, Choi SM, Rhee YM (2013) Simple method for simulating the mixture of atomistic and coarse-grained molecular systems. J Chem Theory Comput 9:3728–3739

Stanley C, Rau D (2011) Evidence for water structuring forces between surfaces. Curr Opin Colloid Interface Sci 16:551–556

Tironi IG, Sperb R, Smith PE, van Gunsteren WF (1995) A generalized reaction field method for molecular dynamics simulations. J Chem Phys 102:5451–5459

Tschöp W, Kremer K, Hahn O, Batoulis J, Bürger T (1998) Simulation of polymer melts. II. From coarse-grained models back to atomistic description. Acta Polym 49:75–79

Tuckerman ME (2010) Statistical mechanics: theory and molecular simulation. Oxford University Press, New York

Uusitalo JJ, Ingólfsson HI, Akhshi P, Tieleman DP, Marrink SJ (2015) Martini coarse-grained force field: extension to DNA. J Chem Theory Comput 11:3932–3945

Villa E, Balaeff A, Mahadevan L, Schulten K (2004) Multiscale method for simulating protein–DNA complexes. Multiscale Model Simul 2:527–553

Villa E, Balaeff A, Schulten K (2005) Structural dynamics of the lac repressor–DNA complex revelead by a multiscale simulation. Proc Natl Acad Sci USA 102:6783–6788

Walther JH, Praprotnik M, Kotsalis EM, Koumoutsakos P (2012) Multiscale simulation of water flow pas a C540 fullerene. J Comput Phys 231:2677–2681

Wang H, Agarwal A (2015) Adaptive resolution simulation in equilibrium and beyond. Eur Phys J Spec Top 224:2269–2287

Wang H, Hartmann C, Schütte C, Delle Site L (2013) Grand-canonical-like molecular-dynamics simulations by using an adaptive-resolution technique. Phys Rev X 3:011018

Wang ZJ, Deserno M (2010) A systematically coarse-grained solvent-free model for quantitative phospholipid bilayer simulations. J Phys Chem B 114:11207–11220

Wassenaar TA, Ingólfsson HI, Böckmann RA, Peter Tieleman DP, Marrink SJ (2015) Computational lipidomics with insane: a versatile tool for generating custom membranes for molecular simulations. J Chem Theory Comput 11:2144–2155

Wassenaar TA, Ingólfsson HI, Priess M, Marrink SJ, Schaefer LV (2013) Mixing martini: electrostatic coupling in hybrid atomistic–coarse-grained biomolecular simulations. J Phys Chem B 117:3516–3530

Yesylevskyy SO, Schäfer LV, Sengupta D, Marrink SJ (2010) Polarizable water model for the coarse-grained MARTINI force field. PLoS Comput Biol 6:e1000810

Young MA, Jayaram B, Beveridge DL (1998) Local dielectric environment of B-DNA in solution: results from a 14 ns molecular dynamics trajectory. J Phys Chem B 102:7666–7669

Zavadlav J (2015) Multiscale simulation of biomolecular systems. PhD thesis, Department of Physics, Faculty of Mathematics and Physics, University of Ljubljana

Zavadlav J, Marrink SJ, Praprotnik M (2016) Adaptive resolution simulation of supramolecular water: the concurrent making, breaking, and remaking of water bundles. J Chem Theory Comput 12:4138–4145

Zavadlav J, Melo MN, Cunha AV, de Vries AH, Marrink SJ, Praprotnik M (2014) Adaptive resolution simulation of martini solvents. J Chem Theory Comput 10:2591–2598

Zavadlav J, Melo MN, Marrink SJ, Praprotnik M (2014) Adaptive resolution simulation of an atomistic protein in martini water. J Chem Phys 140:054114

Zavadlav J, Melo MN, Marrink SJ, Praprotnik M (2015) Adaptive resolution simulation of polarizable supramolecular coarse-grained water models. J Chem Phys 142:244118

Zavadlav J, Podgornik R, Melo MN, Marrink SJ, Praprotnik M (2016) Adaptive resolution simulation of an atomistic DNA molecule in MARTINI salt solution. Eur Phys J Spec Top 225:1595–1607

Zavadlav J, Podgornik R, Praprotnik M (2015) Adaptive resolution simulation of a DNA molecule in salt solution. J Chem Theory Comput 11:5035–5044

Zhou HX (2014) Theoretical frameworks for multiscale modeling and simulation. Curr Opin Struct Biol 25:67–76